



Constraints on the efficiency of the photoelectric heating in a molecular ridge of the metal-poor LMC

L.Belloir, F.Galliano, S.Madden, V.Lebouteiller, M.Varese, and the LMC+ collaboration

CEA PARIS-SACLAY
DEPARTMENT OF ASTROPHYSICS



Introduction

The Large Magellanic Cloud (LMC) provides a unique laboratory to understand the properties of the interstellar medium (ISM) in a half-solar-metallicity galaxy. The LMC's proximity to our Galaxy (d=55 kpc) permits observation of its infrared emission at parsec-scale resolution, thereby enabling study of interstellar dust properties at the scale of a molecular cloud. The SOFIA Legacy Program (LMC+) [8] has mapped the [CII] $\lambda 158\mu m$ and [OIII] $\lambda 88\mu m$ lines in the molecular ridge south of 30 Doradus, at a resolution of 2.5 pc. These new observations trace the emission from the dominant cooling lines in the neutral and ionised ISM, enabling an investigation of the major heating and cooling mechanisms in the three massive star-forming regions, N158, N159 and N160. In neutral regions, the main mechanism responsible for the gas heating is the photoelectric effect. This process consists of the ejection of an electron from a dust grain after the absorption of a UV photon. This photo-electron will subsequently heat the gas through collisions.

STATE OF THE ART

- Photoelectric (PE) heating depends on grain properties (size distribution, composition, solid-state structure, etc.) which are poorly constrained.
- The efficiency of the PE heating has been empirically calibrated on a small number of Galactic regions. [1, 6, 12]
- The effect of metallicity on the PE efficiency is poorly understood. The PE efficiency in extragalactic environment has been studied in the literature, but without the possibility to compare it to the abundance of its carriers, the small grains [7, 11].
- ⇒ Our goal is to relate the PE efficiency to the small grain abundance derived from SED modelling.

OBJECTIVES

- Combining data acquired by the SAGE [10] survey with Spitzer (3.6 to 70 microns), the HERITAGE [9] survey with Herschel (100 to 250 microns), and new data from the LMC+ survey with SOFIA.
- Computing maps of the dust properties (column density $\Sigma_d [M_{\odot}.pc^{-2}]$, mean starlight intensity $\langle U \rangle$, fraction of small grains q_{AF} , total luminosity) from SED modelling.
- Providing the contribution of each phase of the observed [CII] line.
- Comparing the spatially-resolved PE efficiency to the dust properties and local physical conditions.

METHODOLOGY

- Convolution of our multi-wavelength maps to SPIRE 500 μm resolution (36 ").
- Reprojection of all maps using the pixel grid of [CII] map.
- Estimation et propagation of our asymmetric uncertainties and their correlations (*bootstrapping*).
- Fitting the spatially-resolved SEDs with the THEMIS [4, 5] dust model, within the hierarchical Bayesian code, HerBIE [3].
- Creation of dust property maps and estimation of ϵ_{PE} the PE heating efficiency.

REFERENCES

- (1) Bakes, E. L. O.; Tielens, A. G. G. M. *The Astrophysical Journal* **1994**, 427, Publisher: IOP ADS Bibcode: 1994ApJ...427..822B, 822.
- (2) Draine, B. T.; Li, A. ApJ **2007**, 657, Number: 2, 810–837.
- (3) Galliano, F. Monthly Notices of the Royal Astronomical Society **2018**, 476, Number: 2, 1445–1469.
- (4) Jones, A. P.; Fanciullo, L.; Koehler, M.; Verstraete, L.; Guillet, V.; Bocchio, M.; Ysard, N. *A&A* **2013**, *558*, A62.
- (5) Jones, A. P.; Koehler, M.; Ysard, N.; Bocchio, M.; Verstraete, L. *A&A* **2017**, *602*, A46.
- (6) Kimura, H. *Monthly Notices of the Royal Astronomical Society* **2015**, 449, Publisher: OUP ADS Bibcode: 2015MNRAS.449.2250K, 2250–2258.
- (7) Lebouteiller, V.; Cormier, D.; Madden, S. C.; Galametz, M.; Hony, S.; Galliano, F.; Chevance, M.; Lee, M.-Y.; Braine, J.; Polles, F. L.; Requeña-Torres, M. A.; Indebetouw, R.; Hughes, A.; Abel, N. *A&A* **2019**, *632*, A106.
- (8) Madden, S. C.; Consortium, T. L. The LMC+ SOFIA Legacy Program, 2023.
- (9) Meixner, M. et al. *AJ* **2013**, *146*, Number: 3, 62.
- (10) Meixner, M. et al. *AJ* **2006**, *132*, Number: 6, 2268–2288.
- (11) Rubin, D. et al. *A&A* **2009**, *494*, Number: 2, 647–661.
- (12) Wolfire, M. G.; Hollenbach, D.; McKee, C. F.; Tielens, A. G. G. M.; Bakes, E. L. O. *The Astro- physical Journal* **1995**, 443, Publisher: IOP ADS Bibcode: 1995ApJ...443..152W, 152.

ABOUT SOFIA AND THE LMC+ COLLABORATION

• SOFIA:

- A Boeing 747SP, mounted with a 2.5 m telescope, observing perpendicular to the flight plan (Fig. 1).
- 8 possible instruments, including imagers and spectrometers, from the mid-IR to the far-IR.
- Operated from 2013 to 2022

• LMC+:

- SOFIA Joint Legacy Program (LMC+): Used the Far Infrared Field-Imaging Lines Spectrometer (FIFI-LS) instrument to map the whole southern molecular ridge.
- 8 flights in March/April 2022 in order to create the biggest map of the region through [CII] $\lambda 158 \mu m$ and [OIII] $\lambda 88 \mu m$ lines with a 2.5 pc linear resolution.

THE [CII] EMISSION OF THE STUDIED REGION

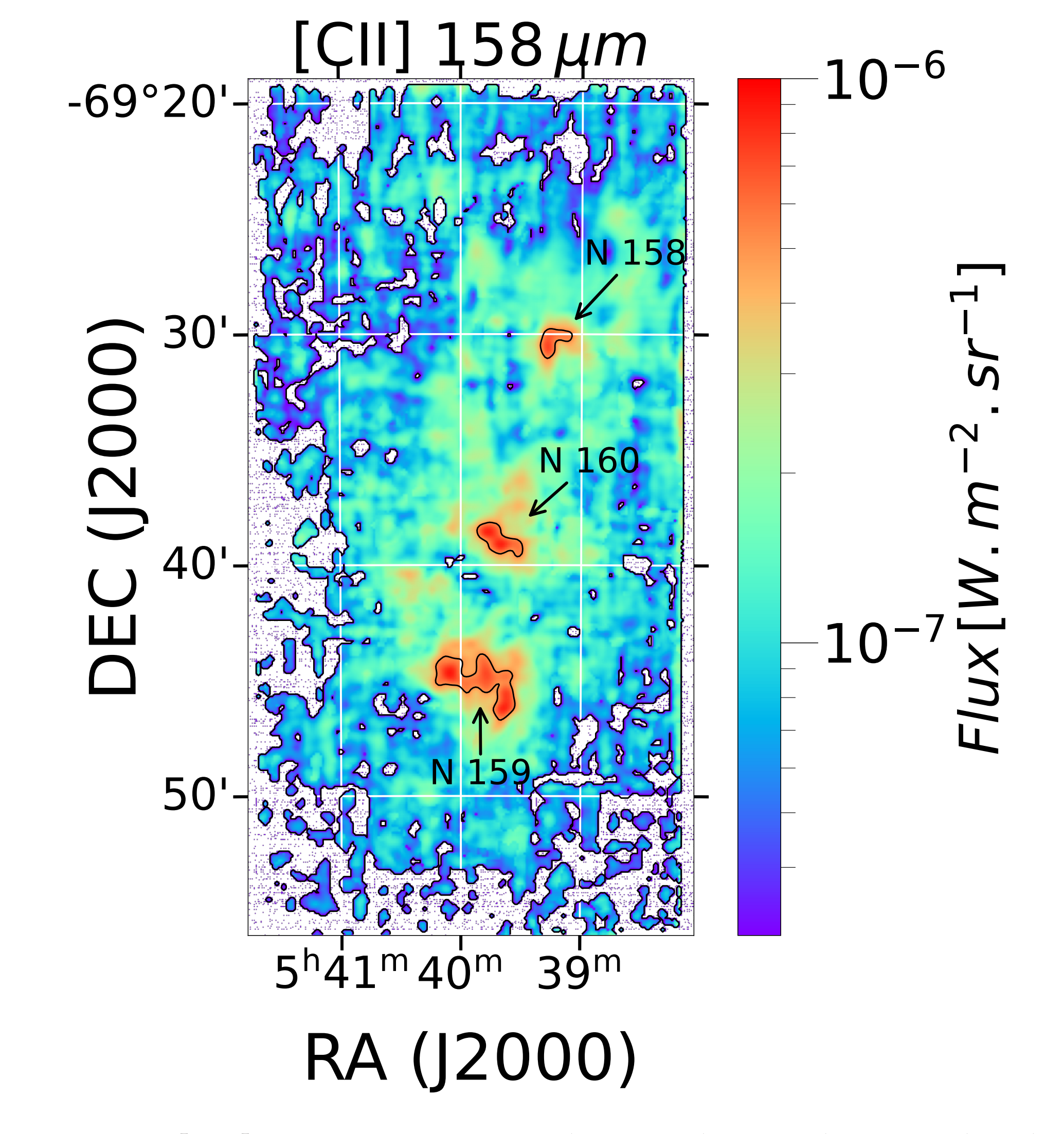


Figure 3: [CII] $\lambda 158 \mu m$ emission line in the southern molecular ridge seen by SOFIA

PHASE DECOMPOSITION

• We can define the [CII] luminosity in the ionized and molecular phase:

$$L_{ion}([CII]) = \alpha_{+}([CII]) = \frac{h\nu_{[CII]}}{n_{crit}^{ion}} \frac{g_{1}}{g_{0}} \left[\frac{C^{+}}{H}\right]^{ion} A_{10} \times \frac{L_{H\alpha}}{h\nu_{H\alpha}\alpha_{H\alpha}} \qquad L_{mol} = \frac{h\nu_{[CII]}}{n_{crit}^{mol}} \frac{g_{1}}{g_{0}} \left[\frac{C^{+}}{H}\right]^{mol} A_{10}N(H_{2})n_{H2}$$
 (1)

With $A_{10} = 2.4 \times 10^{-6} \, s^{-1}$, $10^{-6} \le [C^+/H]^{ion,mol} \le 10^{-4}$ the abundance of ionized carbon in each phase, $\frac{g_1}{g_0} = 2$, $\alpha_{H\alpha}(T = 8000K) = 16 \times 10^{-14} \, cm^3. s^{-1}$, $n_{crit}^{ion}(T = 8000\, K) = 44 \, cm^{-3}$, $n_{crit}^{mol}(T = 100\, K) = 6000 \, cm^{-3}$, $10^2 cm^{-3} \le n_{H2} \le 5 \times 10^5 cm^{-3}$.

• Assuming that the PE heating only dominates in the neutral atomic medium we define the [CII] luminosity attributed to the PE heating as:

$$L_{ato}([CII]) = L_{PE}([CII]) = \epsilon_{PE} L_{AF} = \epsilon_{PE} \beta \langle U \rangle \Sigma_d q_{AF}$$
(2)

With ϵ_{PE} the PE heating efficiency, $\beta = 98/0.17 [L_{\odot}.M_{\odot}^{-1}]$ and L_{AF} the luminosity attributed to the small grains (R<1.5nm).

 \Rightarrow Doing a *bootstrapping*, we compute the PE efficiency without the ionized and molecular contribution of $L_{obs}([CII])$:

$$\epsilon_{PE} \equiv \frac{L_{obs}([CII]) - L_{ion}([CII]) - L_{mol}([CII])}{\beta \langle U \rangle \Sigma_d q_{AF}}$$
(3)

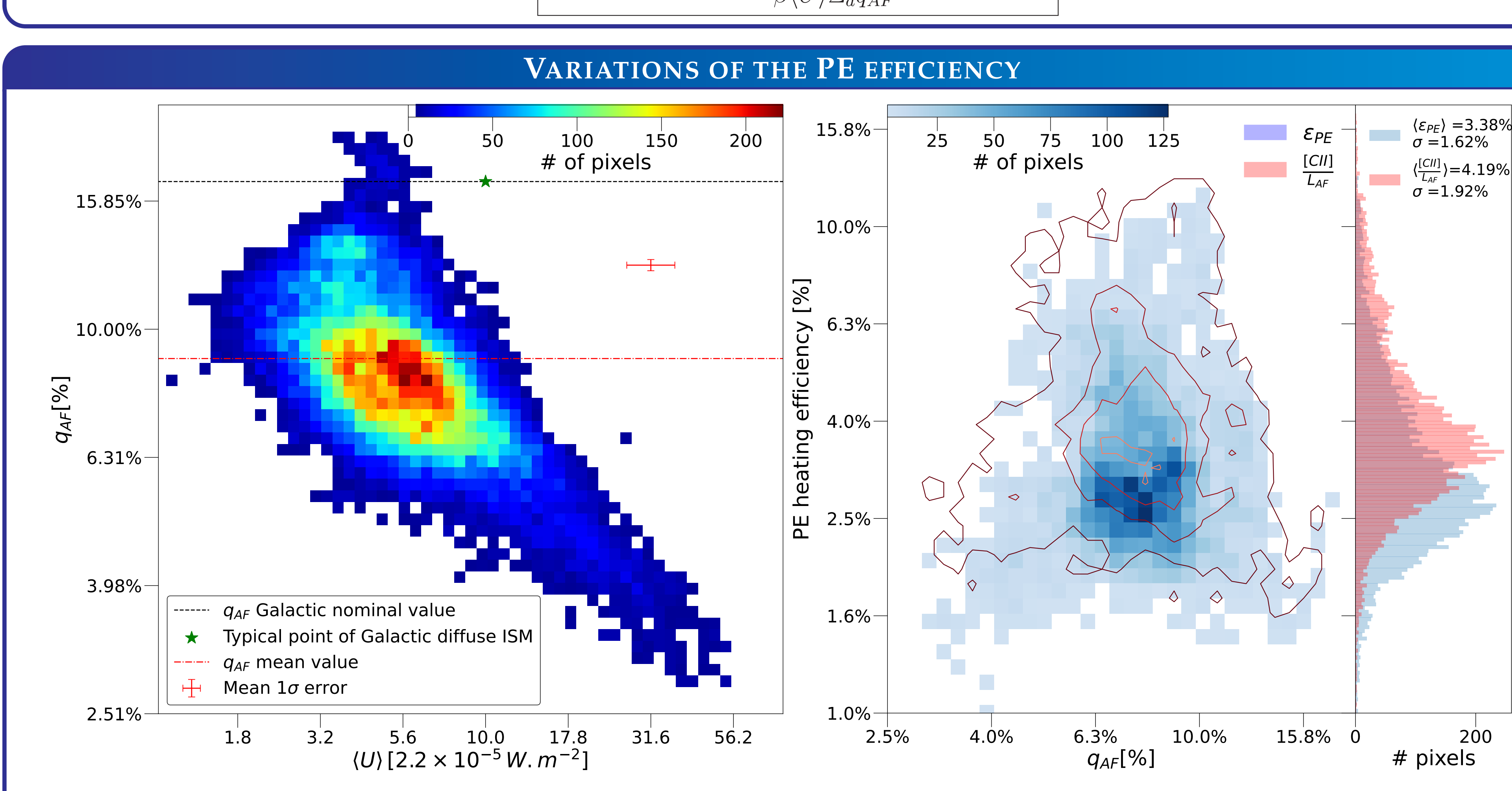


Figure 1: Fraction of small grains (R<1.5nm) versus the mean Interstellar Radiation Field ($\langle U \rangle$, as defined in [2])

Figure 2: The left panel display the PE heating efficiency estimation as a function of the fraction of small grains (R<1.5 nm). The blue take into account the phase decomposition, the red contours do not. We also display on the right panel the pixel's distribution.

MAIN RESULTS

- The PE effect is dominated by small grains.
- Clear correlation between the abundance of the small a-C(:H) grains, the carriers of the PE effect, and the starlight intensity (Fig. 5) \Rightarrow destruction of these carriers by intense stellar radiation.
- Because of the half-solar metallicity, the fraction of small grains in the southern molecular ridge is around 8% (Fig. 6), that is half of the average Galactic value (17%)
- We manage to decompose the contribution of each phase in the [CII] observed luminosity.
- The average efficiency over the map for both methods are $\mu([CII]/L_{AF}) = 1.78^{+2.76}_{-0.03}\%$ and $\mu(\epsilon_{PE}) = 1.42^{+2.20}_{-0.02}\%$.
- The phase decomposition provides a relative correction around 25%
- Next step: Conduct the phase decomposition at 18'' resolution \Rightarrow Stay tuned for the incoming paper.